Nonlinear Processes in Geophysics (1997) 4: 55–62

Nonlinear Processes in Geophysics

Dynamics of large-amplitude geostrophic flows over bottom topography

E.S. Benilov and P.V. Sakov

Department of Applied Computing and Mathematics, University of Tasmania, P.O.Box 1214, Launceston 7250, Australia

Received 9 January 1996 - Revised 4 June 1996 - Accepted 25 November 1996

Abstract. We examine the interaction of near-surface and near-bottom flows over bottom topography. A set of asymptotic equations for geostrophic currents in a three-layer fluid is derived. The depths of the active (top/bottom) layers are assumed small, the slope of the bottom is weak, the interfacial displacement is comparable to the depths of the thinner layers. Using the equations derived, we examine the stability of parallel flows and circular eddies. It is demonstrated that eddies with non-zero near-surface component are always unstable; eddies localized in the near-bottom layer may be stable subject to additional restrictions imposed on their horizontal profiles and bottom topography.

1 Introduction

Flows with large displacement of isopycnal surfaces have received a lot of attention over the past decade; however, many important questions still have no answers. The main difficulty is posed by a large number of governing parameters, resulting in an extreme variety of "species" in the large-amplitude geostrophic "zoo" - each behaving in its own way. A classification of two-layer flows over a flat bottom has been proposed by Benilov and Reznik (1996), but flows over bottom topography seem to manifest different properties. For example, most of large-amplitude zonal currents over a flat bottom are unstable (see Benilov and Reznik (1996) and references therein), while the topography driven regime introduced by Swaters and Flierl (1991) includes a wide class of linearly stable near-bottom currents (Karsten et al., 1996). Furthermore, Karsten and Swaters (1996) demonstrated that some topographic flows are stable with respect to both linear and nonlinear disturbances!

It should be noted, however, that asymptotic equations like those used by Karsten et al. (1996) and Karsten and Swaters (1996) are always subject to criticism that possible instabilities may have been "scaled out" of the problem. In particular, oceanographic observations (e.g. Cooper , 1955; Smith , 1976; Houghton et al., 1982; Zoccolotti and Salusti , 1987; Stasey et al. , 1987) show that near-bottom flows often co-exist with strong near-surface currents, but the equations derived by Swaters and Flierl (1991) did not take into consideration the above-thermocline layer of the ocean. This implies that the passive middle layer "cushions" the surface/bottom interaction. No estimates, however, have been made, and it is unclear how thick the middle layer must be to satisfy this assumption. Judging from a similar problem considered by Killworth (1983) and Killworth et al. (1984), a layer becomes passive only if it is about 100 times thicker than the active layer, which does not seem to hold in the ocean.

This paper examines the effect of near-surface motion on the stability of near-bottom geostrophic flows over topography. The simplest natural setting for this problem is the three-layer (f-plane) model: two active layers and a passive [1] layer in between. The near-bottom layer is assumed thin compared to the total depth of the ocean (which is supported by all above-mentioned observations except Houghton et al. (1982)). The Rossby number is small. A set of geostrophic equations is derived in Sects. 2 and 3, using which the stability of coupled near-surface, near-bottom flows and eddies is examined in Sect. 4.

2 Formulation

Consider a three-layer fluid on the f-plane (Fig. 1). Introducing the spatial coordinates $\mathbf{r}_* = (x_*, y_*)$, the time t_*, the densities ρ_{i*}, the depths h_{i*}, the veloci-

Correspondence to: E.S.Benilov

[1] Here and in what follows, the term "passive" means that the flow in the corresponding layer is weaker than those in the active layers. It may still influence, however, the dynamics of the system

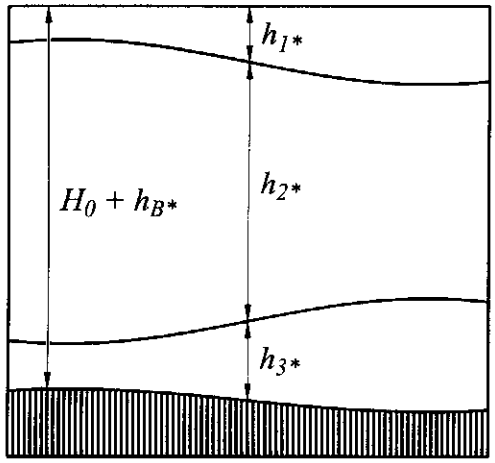

Fig. 1. Geometry of the problem.

ties $\mathbf{u}_{i*} = (u_{i*}, v_{i*})$, and the pressures p_{i*} of the layers ($i = 1, 2, 3$; 1 corresponds to the upper layer), we can write the governing equations in the form

$$\left.\begin{array}{l} \frac{\partial \mathbf{u}_{i*}}{\partial t_*} + (\mathbf{u}_{i*}\nabla)\mathbf{u}_{i*} + \frac{1}{\rho_0}\nabla p_{i*} = f\,\mathbf{u}_{i*} \times \mathbf{k}, \\ \frac{\partial h_{i*}}{\partial t_*} + \nabla(\mathbf{u}_{i*}\, h_{i*}) = 0, \end{array}\right\} \quad (1)$$

where $\mathbf{u} \times \mathbf{k} = (v, -u)$, f is the Coriolis parameter, and ρ_0 is the average density of the fluid (the Boussinesq approximation implied). The pressures are given by the hydrostatic formulae:

$$\left.\begin{array}{l} p_{2*} = p_{1*} - g(\rho_{2*} - \rho_{1*})h_{1*}, \\ p_{3*} = p_{2*} - g(\rho_{3*} - \rho_{2*})(h_{1*} + h_{2*}), \end{array}\right\} \quad (2)$$

where g is the acceleration due to gravity. We shall also use the rigid-lid approximation:

$$h_{1*} + h_{2*} + h_{3*} = H_0 + h_{B*}, \quad (3)$$

where H_0 is the depth scale of the ocean and $h_{B*}(\mathbf{r}_*)$ describes the bottom topography.

Next we introduce

$$\left.\begin{array}{lll} \mathbf{r} = \mathbf{r}_*/L, & t = t_*/T, & \\ \mathbf{u}_i = \mathbf{u}_{i*}/U_i, & p_i = p_{i*}/P_i, & h_i = h_{i*}/H_i, \\ h_B = h_{B*}/H_B, & & \end{array}\right\} \quad (4)$$

where the new (non-dimensional) variables have no asterisks and the corresponding dimensional scales are denoted by capital letters. We assume that the flow is geostrophic, i.e.

$$\frac{1}{\rho_0}\frac{P_i}{L} = fU_i \quad (5)$$

Substitution of Eqs. 4,5 into Eqs. 1-3 yields

$$\epsilon_T \frac{\partial \mathbf{u}_i}{\partial t} + \epsilon_i(\mathbf{u}_i\nabla)\mathbf{u}_i + \nabla p_i = \mathbf{u}_i \times \mathbf{k}, \quad (6)$$

$$\epsilon_T \frac{\partial h_i}{\partial t} + \epsilon_i \nabla(\mathbf{u}_i h_i) = 0, \quad (7)$$

$$\left.\begin{array}{l} \epsilon_L\epsilon_2 p_2 = \epsilon_L\epsilon_1 p_1 - \mu\delta_1 h_1, \\ \epsilon_L\epsilon_3 p_3 = \epsilon_L\epsilon_2 p_2 - \nu(\delta_1 h_1 + \delta_2 h_2), \\ \delta_1 h_1 + \delta_2 h_2 + \delta_3 h_3 = 1 + \delta_B h_B, \end{array}\right\} \quad (8)$$

where

$$\epsilon_i = \frac{U_i}{fL}, \quad (9)$$

$$\delta_i = \frac{H_i}{H_0}, \quad \delta_B = \frac{H_B}{H_0},$$

$$\epsilon_T = \frac{1}{Tf}, \quad \epsilon_L = \frac{L^2 f^2 \rho_0}{g(\rho_{3*} - \rho_{1*})H_0},$$

$$\mu = \frac{\rho_{2*} - \rho_{1*}}{\rho_{3*} - \rho_{1*}}, \quad \nu = \frac{\rho_{3*} - \rho_{2*}}{\rho_{3*} - \rho_{1*}} \quad (10)$$

(observe that $\mu + \nu = 1$). The only "crucial" assumption in our analysis will be

$$\epsilon_i \ll 1, \quad \epsilon_T \ll 1, \quad (11)$$

i.e. the flow is geostrophic. Observe that, in application to flows with large interfacial displacement (which we are interested in), condition 11 also restricts the spatial scale of the flow - see Subsect. 3.1.

Now we can expand Eq. 6 as follows:

$$u_i = -\frac{\partial p_i}{\partial y} - \epsilon_i J\left(p_i, \frac{\partial p_i}{\partial x}\right) - \epsilon_T \frac{\partial^2 p_i}{\partial t \partial x} + O(\epsilon_i^2, \epsilon_T^2, \epsilon_i\epsilon_T),$$

$$v_i = \frac{\partial p_i}{\partial x} - \epsilon_i J\left(p_i, \frac{\partial p_i}{\partial y}\right) - \epsilon_T \frac{\partial^2 p_i}{\partial t \partial y} + O(\epsilon_i^2, \epsilon_T^2, \epsilon_i\epsilon_T),$$

and substitute it into Eq. 7:

$$\epsilon_T \frac{\partial h_i}{\partial t} + \epsilon_i J(p_i, h_i) - \epsilon_i \nabla\left\{h_i\left[\epsilon_i J(p_i, \nabla p_i) + \epsilon_T \frac{\partial \nabla p_i}{\partial t}\right]\right\} = O(\epsilon_i^3, \epsilon_i\epsilon_T^2, \epsilon_i^2\epsilon_T). \quad (12)$$

Next we shall combine Eqs. 12 as $\sum_{i=1}^{3} \delta_i \times$Eq. (12), and obtain

$$\epsilon_T \frac{\partial}{\partial t}\sum_{i=1}^{3}\delta_i h_i + \sum_{i=1}^{3}\epsilon_i\delta_i J(p_i, h_i) - \sum_{i=1}^{3}\delta_i\epsilon_i\nabla\left\{h_i\left[\epsilon_i J(p_i, \nabla p_i) + \epsilon_T \frac{\partial \nabla p_i}{\partial t}\right]\right\} = O(\delta_i\epsilon_i^3, \delta_i\epsilon_i\epsilon_T^2, \delta_i\epsilon_i^2\epsilon_T). \quad (13)$$

Rewriting Eq. 8 as

$$p_1 = \frac{\epsilon_2}{\epsilon_1}p_2 + \mu\frac{1}{\epsilon_L\epsilon_1}\delta_1 h_1, \quad (14)$$

$$p_3 = \frac{\epsilon_2}{\epsilon_3}p_2 - \nu\frac{1}{\epsilon_L\epsilon_3}(1 + \delta_B h_B - \delta_3 h_3), \quad (15)$$

$$h_2 = \frac{1}{\delta_2}(1 + \delta_B h_B - \delta_1 h_1 - \delta_3 h_3), \quad (16)$$

we substitute these equalities into the first two terms of Eq. 13:

$$-\nu\frac{\delta_3\delta_B}{\epsilon_L}J(h_B, h_3) + \epsilon_2\delta_B J(p_2, h_B) - \sum_{i=1}^{3}\delta_i\epsilon_i\nabla\left\{h_i\left[\epsilon_i J(p_i, \nabla p_i) + \epsilon_T \frac{\partial \nabla p_i}{\partial t}\right]\right\} = O(\delta_i\epsilon_i^3, \delta_i\epsilon_i\epsilon_T^2, \delta_i\epsilon_i^2\epsilon_T). \quad (17)$$

This equation will replace the h_2-equation in Eq. 12. The remaining two equations can be rewritten, using Eqs. 14–16, in the form

$$\epsilon_T \frac{\partial h_1}{\partial t} + \epsilon_2 J(p_2, h_1) = O(\epsilon_1^2, \epsilon_1\epsilon_T), \tag{18}$$

$$\epsilon_T \frac{\partial h_3}{\partial t} + \epsilon_2 J(p_2, h_3) - \nu\frac{\delta_B}{\epsilon_L} J(h_B, h_3) = O(\epsilon_3^2, \epsilon_3\epsilon_T). \tag{19}$$

Equations 14–19 form a closed system for $p_{1,2,3}$ and $h_{1,2,3}$.

3 Asymptotic analysis

Geostrophic equations 14–19 are much simpler than the original system (1) and can be, to a certain extent, analyzed for any values of the parameters involved. From a physical viewpoint, however, further analysis would be facilitated by fixing the orders of ϵ_i, δ_i etc. - otherwise we shall be lost in tens of possible regimes.

First of all, we assume that

$$\delta_B \ll 1,$$

which means that either the depth variations are weak compared to the average depth of the ocean, or the slope of the bottom is small compared to the slopes of the layers' interfaces. If this condition does not hold, the flow is dominated by topography (e.g. Pedlosky 1987) and the problem becomes trivial. We shall also assume the depth of the lower layer to be much smaller than the total depth of the ocean:

$$\delta_3 \ll 1,$$

which is both relevant physically (see Cooper 1955, Smith 1976, Zoccolotti and Salusti 1987) and interesting mathematically (a thin layer is more "sensitive" to the bottom topography, resulting richer dynamics). On the other hand, the middle layer should be assumed thick:

$$\delta_2 = 1, \tag{20}$$

otherwise the upper layer would be the only thick layer and the flow would become barotropic. Baroclinicity of the flow implies two further conditions: given that the pressures in the layers are different, the last terms in Eqs. 14,15 must be of order one:

$$\frac{\delta_1}{\epsilon_L\epsilon_1} = 1, \tag{21}$$

$$\frac{\delta_B}{\epsilon_L\epsilon_3} = 1 \quad \text{or} \quad \frac{\delta_3}{\epsilon_L\epsilon_3} = 1 \tag{22}$$

(it should be recalled here that $\mu, \nu = O(1)$ - see Eq. 10).

We need another 3 conditions to fix the parameters involved. Purporting to derive the most general equations (i.e. retain as many terms as possible), we require that

(i) the last two terms in Eq. 15 be of the same order:

$$\delta_B = \delta_3; \tag{23}$$

(ii) the topography and passive-layer terms in Eq. 19 be of the same order:

$$\epsilon_2 = \frac{\delta_B}{\epsilon_L}; \tag{24}$$

(iii) the topography and the first two nonlinear terms in Eq. 17 be of the same order:

$$\frac{\delta_3\delta_B}{\epsilon_L} = \delta_1\epsilon_1^2 = \delta_2\epsilon_2^2. \tag{25}$$

(We do not require the nonlinear term $\sim \delta_3\epsilon_3$ to be necessarily retained in Eq. 17 — this equation "includes" the third layer through the topography term.) Finally, Eqs. 18,19 show that

$$\epsilon_T = \epsilon_2. \tag{26}$$

Solving Eqs. 20–26, we express $\epsilon_T, \epsilon_{1,2,3}$ and $\delta_{1,2,3}$ through δ_B:

$$\left.\begin{array}{llll} \epsilon_T = \delta_B, & \epsilon_L = 1, & & \\ \epsilon_1 = \delta_B^{2/3}, & \epsilon_2 = \epsilon_3 = \delta_B, & & \\ \delta_1 = \delta_B^{2/3}, & \delta_2 = 1, & \delta_3 = \delta_B. & \end{array}\right\} \tag{27}$$

Substituting Eqs. 27 into Eqs. 14–19 and keeping the leading-order terms only, we can rewrite the governing equations in the form

$$\frac{\partial h_1}{\partial t} + J(p_2, h_1) = 0, \tag{28}$$

$$\frac{\partial \nabla^2 p_2}{\partial t} + J(p_2, \nabla^2 p_2) + \mu^2\nabla[h_1 J(h_1, \nabla h_1)] = J(\nu h_3 + p_2, h_B), \tag{29}$$

$$\frac{\partial h_3}{\partial t} + J(p_2 - h_B, h_3) = 0. \tag{30}$$

Eqs. 28–30 form a closed set for h_1, p_2 and h_3. The set used by Karsten et al. (1996) and Karsten and Swaters (1996) in their stability analyses follows from Eqs. 28–30 if $h_1 = \text{const}$, $\mu = 0$, $\nu = 1$.

3.1 Discussion

(i) We also note that Eqs. 28–30 should not be expected to correctly describe *short* disturbances. The reason for that is that the condition of geostrophy 11 restricts, in fact, the spatial scale of the flow. Indeed, substituting Eq. 9 into Eq. 11:

$$\frac{U_i}{fL} \ll 1, \tag{31}$$

we take into account the geostrophic relation:

$$U_i = \frac{\delta P_i}{Lf}, \tag{32}$$

where δP_i is the pressure variation in the i-th layer. It can be readily seen that conditions 31,32 are most restrictive for $i = 1$ (the flow in the top layer is the strongest). Estimating

$$\delta P_1 = g(\rho_{2*} - \rho_{1*})\delta H_1, \tag{33}$$

and further

$$\delta H_1 = H_1 \tag{34}$$

(the displacement of the interface is of the order of the layer's thickness), we can reduce condition 31 to

$$\frac{L^2}{R_{d1}^2} \gg 1, \tag{35}$$

where

$$R_{d1} = \frac{\sqrt{g(\rho_{2*} - \rho_{1*})H_1}}{f}.$$

Thus, the horizontal spatial scale of the flow must be much larger than the deformation radius based on the parameters of upper layer.

(ii) Finally, we note that the accuracy of Eqs. 28–30 is not very high: some of the omitted terms were only δ_B times smaller than the terms retained, e.g.

$$\delta_1\epsilon_1\nabla\left(h_1\frac{\partial\nabla p_1}{\partial t}\right) \quad \text{was omitted,}$$

$$\delta_2\epsilon_2\nabla\left(h_2\frac{\partial\nabla p_2}{\partial t}\right) \quad \text{was retained.}$$

Thus, the system 28-30 should be looked at as a rough, qualitative model — we shall use it only to demonstrate the importance of near-surface dynamics for near-bottom flows.

4 Stability of parallel flows and eddies

Introducing a new variable

$$f_1 = \frac{2}{3}h_1^{2/3}, \tag{36}$$

we rewrite Eqs. 28–30 as

$$\left.\begin{array}{l} \frac{\partial f_1}{\partial t} + J(p_2, f_1) = 0, \\ \frac{\partial\nabla^2 p_2}{\partial t} + J(p_2, \nabla^2 p_2) + \mu^2 J(f_1, \nabla^2 f_1) \\ \qquad\qquad = J(\nu h_3 + p_2, h_B), \\ \frac{\partial h_3}{\partial t} + J(p_2 - h_B, h_3) = 0. \end{array}\right\} \tag{37}$$

Eqs. 37 admit a steady solution describing a parallel flow over one-dimensional topography ("ridge"or "gorge"):

$$f_1 = \bar{f}_1(y),\ p_2 = \bar{p}_2(y),\ h_3 = \bar{h}_3(y),\ h_B = h_B(y), \tag{38}$$

and a circular eddy over radially symmetric topography ("mountain" or "dip"):

$$f_1 = \bar{f}_1(r),\ p_2 = \bar{p}_2(r),\ h_3 = \bar{p}_3(r),\ h_B = h_B(r), \tag{39}$$

where $r = \sqrt{x^2 + y^2}$ and the bar marks parameters of the mean flow.

In this section, we shall examine the stability of solutions 38,39.

4.1 Parallel flows

We linearize the governing equations, i.e. substitute

$$f_1 = \bar{f}_1(y) + f_1'(x,y,t), \qquad p_2 = \bar{p}_2(y) + p_2'(x,y,t),$$
$$h_3 = \bar{h}_3(y) + h_3'(x,y,t), \qquad h_B = h_B(y)$$

into Eqn. 37 and omit nonlinear terms:

$$\begin{array}{l} \frac{\partial f_1'}{\partial t} + \frac{\partial p_2'}{\partial x}\frac{\partial \bar{f}_1}{\partial y} - \frac{\partial \bar{p}_2}{\partial y}\frac{\partial f_1'}{\partial x} = 0, \\ \frac{\partial\nabla^2 p_2'}{\partial t} + \frac{\partial p_2'}{\partial x}\frac{\partial\nabla^2\bar{p}_2}{\partial y} - \frac{\partial\bar{p}_2}{\partial y}\frac{\partial\nabla^2 p_2'}{\partial x} \\ \qquad +\mu^2\left(\frac{\partial f_1'}{\partial x}\frac{\partial\nabla^2\bar{f}_1}{\partial y} - \frac{\partial\bar{f}_1}{\partial y}\frac{\partial\nabla^2 f_1'}{\partial x}\right) = \left(\nu\frac{\partial h_3'}{\partial x} + \frac{\partial p_2'}{\partial x}\right)\frac{\partial h_B}{\partial y}, \\ \frac{\partial h_3'}{\partial t} + \frac{\partial p_2'}{\partial x}\frac{\partial\bar{h}_3}{\partial y} - \frac{\partial\bar{p}_2}{\partial y}\frac{\partial h_3'}{\partial x} + \frac{\partial h_B}{\partial y}\frac{\partial h_3'}{\partial x} = 0. \end{array}$$

Assuming the harmonic dependence of the disturbance on x and t:

$$f_1'(x,y,t) = \phi(y)\exp[ik(ct-x)],$$
$$p_2'(x,y,t) = \chi(y)\exp[ik(ct-x)],$$
$$h_3'(x,y,t) = \eta(y)\exp[ik(ct-x)],$$

where k and c are the wavenumber and phase speed, we obtain

$$(c-U_2)\phi + \frac{1}{\mu}U_1\chi = 0, \tag{40}$$

$$(c-U_2)\left(\frac{d^2\chi}{dy^2} - k^2\chi\right) + \frac{d^2U_2}{dy^2}\chi - \mu U_1\left(\frac{d^2\phi}{dy^2} - k^2\phi\right) + \mu\frac{d^2U_1}{dy^2}\phi + S(\nu\eta + \chi) = 0 \tag{41}$$

$$(c - U_2 - S)\eta + \frac{1}{\nu}U_3\chi = 0, \tag{42}$$

where

$$U_1 = -\mu\frac{d\bar{f}_1}{dy}, \quad U_2 = -\frac{d\bar{p}_2}{dy}, \quad U_3 = -\nu\frac{d\bar{h}_3}{dy}, \quad S = \frac{dh_B}{dy}.$$

Next, the substitution

$$\phi = \frac{1}{\mu}U_1\psi, \quad \chi = -(c-U_2)\psi, \quad \eta = \frac{1}{\nu}\frac{(c-U_2)U_3}{c-U_2-S}\psi \tag{43}$$

reduces Eqs. 40–42 to a single equation for the new unknown ψ:

$$\frac{d}{dy}\left\{\left[(c-U_2)^2 + U_1^2\right]\frac{d\psi}{dy}\right\} - \left\{k^2\left[(c-U_2)^2 + U_1^2\right] + \frac{S(c-U_2)U_3}{c-U_2-S} - S(c-U_2)\right\}\psi = 0. \tag{44}$$

Eq. 44 will be considered in a zonal channel, i.e.

$$\psi = 0 \quad \text{at} \quad y = d_{1,2}, \tag{45}$$

which follows from the no-flow boundary conditions at the walls of the channel located at $y = d_{1,2}$. If there is no motion in the upper layers,

$$U_{1,2} = 0, \qquad S \neq 0, \tag{46}$$

the solution to Eqs. 44–45 is stable provided

$$U_3 \leq 0 \tag{47}$$

(Karsten et al., 1996). In the opposite limiting case,

$$U_{1,2} \neq 0, \qquad S = 0, \tag{48}$$

U_3 cancels out and Eq. 44 becomes equivalent to the two-layer equation, which was found unstable by Benilov (1992). Thus, in the general case, we have two competing influences: bottom topography (sometimes) stabilizes near-bottom flows, while motion in the upper layers makes them unstable. Which influence prevails?

Unfortunately, this question cannot be answered rigorously, as the integral approach, which Karsten et al. (1996) and Benilov (1992) used for Eq. 46 and Eq. 48 respectively, in the general case becomes inconclusive (see a similar result for eddies in Subsect. 4.3. We can observe, however, that the destabilizing term in Eq. 44 is proportional to k^2, while the stabilizing terms ($\sim S$) remain finite as $k \to \infty$. Thus it can be conjectured that *short* disturbances are not "sensitive" to the topography and are always unstable!

In order to illustrate this conjecture, we consider the eigenvalue problem (44,45) with

$$U_{1,2,3} = \text{const}, \qquad S = \text{const},$$

i.e. the slopes of $h_{2,3}$ and h_B are constants, while the depth of the upper layer is

$$h_1 = \text{const} y^{2/3}$$

[see formula (4.1)]. The eigenfunction ψ, in this case, is given by sine or cosine, and c satisfies the following dispersion equation:

$$(c - U_2 - S)\left\{K^2\left[(c-U_2)^2 + U_1^2\right] - S(c-U_2)\right\} + S(c-U_2)U_3 = 0, \tag{49}$$

where

$$K^2 = k^2 + \left(\frac{n\pi}{2d}\right)^2.$$

In the short-wave limit

$$K^2 \gg \frac{|S(c-U_2)|}{U_1^2} \max\left\{1, \frac{|U_3|}{|c-U_2-S|}\right\}, \tag{50}$$

the term in square brackets in Eq. 49 dominates the other terms, and one of the three modes described by Eq. 49,

$$c \approx U_2 - i|U_1|, \tag{51}$$

is unstable.

4.2 Discussion

(i) Dispersion relation 51 was derived in the short-wave limit of asymptotic system 28–30, thus we should ensure that short disturbances satisfy the applicability condition 35 of the latter. First, we substitute Eq. 51 into Eq. 50:

$$K^2 \gg \frac{|S|}{U_1} \max\left\{1, \frac{|U_3|}{|iU_1 - S|}\right\}.$$

Assuming for simplicity that all parameters of the flow are of the same order: $|U_1| \sim |U_3| \sim |S|$ (which is consistent with our scaling), we obtain

$$K^2 \gg 1,$$

or, in the dimensional form,

$$\lambda_*^2 \ll R_{d0}^2,$$

where λ_* is the wavelength of the disturbance and

$$R_{d0} = \frac{\sqrt{g(\rho_{3*} - \rho_{1*})H_0}}{f}$$

is the deformation radius based on the global parameters of the fluid. At the same time, λ_* should satisfy the applicability condition 35. Rewriting the latter in the form

$$\lambda_*^2 \gg R_{d1}^2,$$

we see that Eqs. 35 and 50 are consistent only if

$$R_{d1}^2 \ll R_{d0}^2.$$

Substituting R_{d0} and R_{d1}, we obtain

$$(\rho_{2*} - \rho_{1*})H_1 \ll (\rho_{3*} - \rho_{1*})H_0,$$

which agrees with our original assumption: the upper layer must be thin. Note also that the instability is proven only for a narrow spectral band characterized by

$$R_{d1}^2 \ll \lambda_*^2 \ll R_{d0}^2,$$

which is, however, enough to prove the overall instability of the flow.

(ii) Observe that the growth rate $\gamma = k\,\mathrm{Im}(c)$ with c given by Eq. 51 blows up in the short-wave limit:

$$\gamma \to k|U_1| \to \infty \quad \text{as} \quad k \to \infty.$$

This is a general feature of asymptotic equations for large-amplitude geostrophic flows with weak or no β-effect (see Tai and Niiler , 1985; Young and Chen , 1996; Benilov and Reznik , 1996, and references therein). The blow-up occurs because Eqs. 28–30 incorrectly describe short disturbances – see restriction 35. In other words, Eqs. 28–30 enable us to establish the fact of instability, but do not describe all of its parameters (i.e. the short-wave cutoff).

(iii) It is also worth observing that, although the instability is caused by the flow in the *top* layer, the amplitude of the disturbance in the *bottom* layer is not necessarily small. Equalities 43 demonstrate that

$$\frac{\eta}{U_3} = \frac{\mu}{\nu}\frac{U_2 - c}{U_2 - c + S}\frac{\phi}{U_1},$$

and the disturbance has comparable amplitudes in the top and bottom layers unless $\mu|U_2 - c| \ll \nu|S|$.

4.3 Circular eddies

Our motivation for this part of the work is twofold:

- firstly, eddies can be used as a further test for the hypothesis about the unstable nature of Eqs. 37.
- secondly, stable eddies could provide a possible "final" result of the instability of near-bottom flows. If no stable eddies exist, the energy of the flow is subject to further depletion into small scales.

We shall assume the topography in Eqs. 37 to be radially symmetric, which can model a dip or a mountain on the ocean bed. (Intuitively, the former seems to constrain disturbances, while the latter seems to destabilize them.) First we shall derive the stability eigenvalue problem (similar to Eqs. 44,45) and discuss those limiting cases where stability or instability can be proven rigorously. Then, we shall illustrate the general conclusions by an example.

Introducing polar variables (r, θ):

$$x = r\cos\theta, \qquad y = r\sin\theta,$$

we linearize Eqs. 37 against the background of Eq. 39 and seek a solution of the form

$$f_1'(r,\theta,t) = \phi(r)\exp[in(ct-\theta)],$$
$$p_2'(r,\theta,t) = \chi(r)\exp[in(ct-\theta)],$$
$$h_3'(r,\theta,t) = \eta(r)\exp[in(ct-\theta)],$$

where n is the azimuthal wavenumber and c is the angular phase speed. Reducing the resulting set to a single equation by the substitution

$$\phi = \frac{1}{\mu}r\Omega_1\psi, \quad \chi = -r(c-\Omega_2)\psi, \quad \eta = \frac{1}{\nu}r\frac{(c-\Omega_2)\Omega_3}{c-\Omega_2-Q}\psi$$

where

$$\Omega_1 = -\mu\frac{1}{r}\frac{d\bar{f}_1}{dr}, \qquad \Omega_2 = -\frac{1}{r}\frac{d\bar{p}_2}{dr},$$
$$\Omega_3 = -\nu\frac{1}{r}\frac{d\bar{h}_3}{dr}, \qquad Q = \frac{1}{r}\frac{dh_B}{dr}. \tag{52}$$

we obtain

$$\frac{d}{dr}\left\{r^3\left[(c-\Omega_2)^2+\Omega_1^2\right]\frac{d\psi}{dr}\right\} - \left[(n^2-1)rB + r^3\frac{Q(c-\Omega_2)\Omega_3}{c-\Omega_2-Q} - r^3Q(c-\Omega_2)\right]\psi = 0, \tag{53}$$

The boundary conditions follow from the requirement that the pressure ϕ be a well-behaved function:

$$r\psi \to 0 \quad \text{as} \quad r \to 0, \infty. \tag{54}$$

Next we multiply Eq. 53 by the complex conjugate of ψ and integrate over $0 < r < \infty$. Taking into account Eq. 54, we obtain

$$\int_0^\infty \left\{r\left[(c-\Omega_2)^2+\Omega_1^2\right]\left[r^2\left|\frac{d\psi}{dr}\right|^2 + (n^2-1)|\psi|^2\right] + r^3Q(c-\Omega_2)\left(\frac{\Omega_3}{c-\Omega_2-Q}-1\right)|\psi|^2\right\}dr = 0. \tag{55}$$

If $Q = 0$ (flat bottom), Eq. 55 yields

$$\int_0^\infty r\left[(c-\Omega_2)^2+\Omega_1^2\right]\left[r^2\left|\frac{d\psi}{dr}\right|^2 + (n^2-1)|\psi|^2\right]dr = 0,$$

which shows that c may not be real (i.e. Eqs. 53,54 with $Q = 0$ may have only unstable solutions). The opposite limiting case

$$\Omega_{1,2} = 0, \qquad S \neq 0$$

(no current in the upper layers) yields

$$\int_0^\infty \left\{rc\left[r^2\left|\frac{d\psi}{dr}\right|^2 + (n^2-1)|\psi|^2\right] + r^3Q\left(\frac{\Omega_3}{c-Q}-1\right)|\psi|^2\right\}dr = 0.$$

Separating the imaginary and real parts, we obtain

$$(\mathrm{Im}\, c)\int_0^\infty \left[r^3\left|\frac{d\psi}{dr}\right|^2 + (n^2-1)r|\psi|^2 - r^3\frac{Q_3\Omega}{|c-Q|^2}|\psi|^2\right]dr = 0.$$

Evidently, a sufficient condition for stability ($\mathrm{Im}\, c = 0$) is

$$Q\Omega_3 \leq 0. \tag{56}$$

Eq. 56 is the exact analogue of condition 47 derived for parallel flows. Substituting Eq. 52 into Eq. 56, we obtain

$$\frac{dh_B}{dr}\frac{d\bar{h}_3}{dr} \geq 0. \tag{57}$$

Examples of eddies satisfying and not satisfying condition 57 are shown in Figs. 2 and 3.

Thus, we have exactly the same situation as in the case of parallel flows: a flow in the upper layer (always) destabilizes near-bottom eddies, while topography (sometimes) makes them stable. In order to find out, which effect dominates in the general case, we observe that the destabilizing term in Eq. 53 is (as before) proportional to the wavenumber. We conclude that short disturbances ($n \to \infty$) are always unstable.

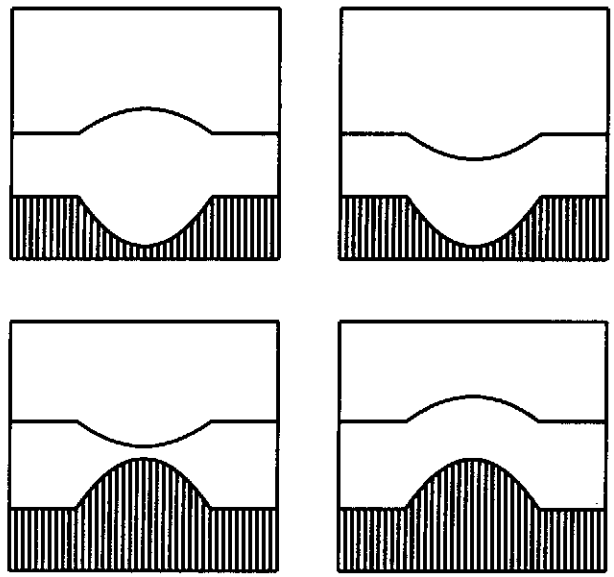

Fig. 2. Stable eddies

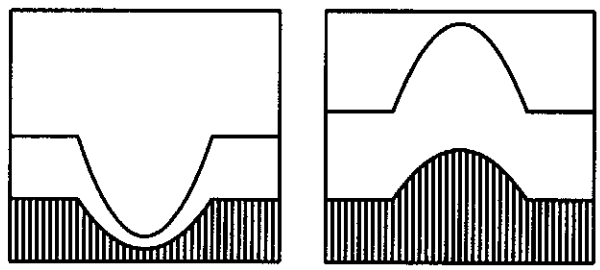

Fig. 3. Potentially unstable eddies

In order to illustrate this conclusion, we consider the example of parabolic eddy over parabolic topography:

$$f_1, p_2, h_3 = \begin{cases} \alpha_{1,2,3} - \frac{1}{2}\Omega_{1,2,3} r^2 & \text{if} \quad r \le a, \\ \alpha_{1,2,3} - \frac{1}{2}\Omega_{1,2,3} a^2 & \text{if} \quad r > a, \end{cases} \tag{58}$$

$$h_B = \begin{cases} \alpha_B - \frac{1}{2}\Omega_{1,2,3} r^2 & \text{if} \quad r \le a, \\ \alpha_B - \frac{1}{2}\Omega_{1,2,3} a^2 & \text{if} \quad r > a, \end{cases} \tag{59}$$

in which case Eq. 53 can be reduced to Bessel's equation. (Eqs. 58,59 imply that $\alpha_{1,3} \ge \frac{1}{2}\Omega_{1,3} a^2$, so that f_1 and h_3 are positive.) Introducing

$$\Psi = r\psi, \qquad C = c - \Omega_2, \tag{60}$$

we substitute Eqs. 58–60 into Eqs. 53,54:

$$(C^2 + \Omega_1^2)\left(r^2 \frac{d^2\Psi}{dr^2} + r\frac{d\Psi}{dr} - n^2\Psi\right) + CQ\left(\frac{\Omega_3}{C-Q} - 1\right) r^2\Psi = 0 \quad \text{if} \quad r < a. \tag{61}$$

$$(C^2 + \Omega_1^2)\left(r^2 \frac{d^2\Psi}{dr^2} + r d\Psi dr - n^2\Psi\right) = 0 \quad \text{if} \quad r > a. \tag{62}$$

$$\Psi \to 0 \quad \text{as} \quad r \to 0, \infty. \tag{63}$$

The solution to Eq. 61–63 (for $n > 0$) is

$$\Psi = J_n\left(\frac{r}{r_0}\right) \quad \text{if} \quad r < a, \tag{64}$$

$$\Psi = A\left(\frac{r}{r_0}\right)^{-n} \quad \text{if} \quad r > a, \tag{65}$$

where J_n is the Bessel function, A is a constant, and

$$\frac{1}{r_0} = \frac{CQ}{C^2 + \Omega_1^2}\left(\frac{\Omega_3}{C-Q} - 1\right). \tag{66}$$

Matching Eqs. 64 and 65 at $r = a$

$$J_n\left(\frac{a}{r_0}\right) = A\left(\frac{a}{r_0}\right)^{-n}, \quad \frac{1}{r_0} J'\left(\frac{a}{r_0}\right) = -nA\frac{1}{r_0}\left(\frac{a}{r_0}\right)^{-n-1}$$

and using the standard identity for the derivative of a Bessel function, we obtain

$$J_{n-1}\left(\frac{a}{r_0}\right) = 0. \tag{67}$$

The dispersion relation 66,67 can be rearranged as follows:

$$\left(\frac{\xi_{n-1,m}}{a}\right)^2 = \frac{CQ}{C^2 + \Omega_1^2}\left(\frac{\Omega_3}{C-Q} - 1\right), \tag{68}$$

where $\xi_{n-1,m}$ is the m-th root of $J_{n-1}(\xi)$. Given that

$$\xi_{n-1,m} \to \infty \quad \text{as} \quad n \to \infty,$$

the three roots of 68 are

$$C \to \pm i\Omega_1, Q \quad \text{as} \quad n \to \infty,$$

which shows that the flow is unstable. Observe that, if there is no flow in the upper layer: $\Omega_1 = 0$, Eq. 68 becomes quadratic and, for certain values of Ω_3 and S, can be shown to have stable roots.

Finally, we note that near-bottom eddies were observed in reality: in an objective analysis of streamfunction maps, Stasey et al. (1988) concluded that there was enough evidence for the formation of subsurface eddies in the Strait of Georgia (Canada). Although the eddies were observed in a "dip" (i.e. exactly where the present analysis predicts them to be stable), we cannot claim the agreement of the theoretical and experimental results, as the eddies were not "sitting" in the dip, but drifting across it.

5 Conclusions

Thus, we have examined the interaction of near-surface and near-bottom large-amplitude currents over topography. Assuming that the Rossby number is small, we derived a set of equations 28–30 for geostrophic flows in a three-layer fluid (Sect. 2,3. The depths of the active (top/bottom) layers were assumed small, the slope of the bottom was weak (otherwise the interaction of the layers and topography would be trivial). Using the equations derived, we examined the stability of parallel flows and circular eddies. It has been demonstrated that

- flows/eddies with non-zero near-surface component are always unstable (Sect. 4.1,4.3);
- even in the cases where the instability is mainly caused by the flow in the top layer, the unstable disturbances may "penetrate" down to the bottom (end of Sect. 4.1);
- flows/eddies localized in the near-bottom layer may be stable subject to additional restrictions imposed on their horizontal profiles and bottom topography (conditions 47 and 56).

It should be emphasized that Eqs. 28–30 are inapplicable to disturbances with wavelengths comparable to the deformation radius R_{d1} based on the depth of the upper layer (see restriction 35). Therefore, we could demonstrate instability in a fairly narrow spectral band, but were unable to calculate the wavelength of maximum growth (which seems to be of the order of R_{d1}). Given that the quasigeostrophic approximation is also inapplicable to the problem at hand (the displacement of isopycnal surfaces in the flow is *large*), the wavelength of maximum growth can only be found using the primitive equations.

References

Benilov, E.S., Large-amplitude geostrophic dynamics: the two-layer model. *Geophys. Astrophys. Fluid Dyn.*, *66*, 67–79, 1992.

Benilov, E.S. and Reznik, G.M., The complete classification of large-amplitude geostrophic flows. *Geophys. Astrophys. Fluid Dyn.*, in print.

Cooper, L.H.N., Deep water movements in the North Atlantic as a link between climatic changes around Iceland and biological productivity of the English Channel and Celtic Sea. *J. Mar. Res.*, *14*, 347–362, 1955.

Houghton, R.W., Schlitz, R., Beardsley, R.C., Butman, B. and Chamberlin, J.L., The Middle Atlantic Bight cold pool: Evolution of the temperature structure during summer 1979. *J. Phys. Oceanogr.*, *12*, 1019-1029, 1982.

Karsten, R.H. and Swaters, G.E., Nonlinear stability of baroclinic fronts in a channel with variable topography. *Stud. Appl. Math.*, in print.

Karsten, R.H., Swaters, G.E.and Thomson, R.E, Stability characteristics of deep water replacement in the Strait of Georgia. *J. Phys. Oceanogr.*, submitted.

Killworth, P.D., Long-wave instability of an isolated front. *Geophys. Astrophys. Fluid Dyn.*, *25*, 235–258, 1983.

Killworth, P.D., Paldor, N. and Stern, M.E. Wave propagation and growth on a surface front in a two-layer geostrophic current. *J. Mar. Res.*, *42*, 761–785, 1984.

Pedlosky, J., *Geophysical Fluid Dynamics*. Springer-Verlag.

Smith, P.C., Baroclinic instability in the Denmark Strait overflow. *J. Phys. Oceanogr.*, *6*, 355–371, 1976.

Stasey, M.W., LeBlond, P.H., Pond, S., Freeland, H.J. and Farmer, D.M., An analysis of the low-frequency current fluctuation in the Strait of Georgia, from June 1984 until January 1985. *J. Phys. Oceanogr.*, *17*, 326–342, 1987.

Stasey, M.W., Pond, S. and LeBlond, P.H., An objective analysis of the low-frequency currents in the Strait of Georgia. *Atmos.-Ocean*, *26*, 1–15, 1988.

Tai, C.K. and Niiler, P.P. Modeling large-scale instabilities in the Kuroshio extension. *Dyn. Atmos. Oceans*, *9*, 359–382, 1985.

Swaters, G.E. and Flierl, G.R., Dynamics of ventilated coherent cold eddies on a sloping bottom. *J. Fluid Mech.*, *223*, 565–587, 1991.

Young, W.R. and Chen, L. Baroclinic instability and thermohaline gradient alignment in the mixed layer. *J. Phys. Oceanogr.*, submitted.

Zoccolotti, L. and Salusti, E. Observations on a very dense marine water in the Southern Adriatic Sea. *Continent. Shelf Res.*, *7*, 535-551, 1987.